Jurnal Mekanikal
Jun 2002, Bil. 13, 11- 25

FINITE ELEMENT ANALYSIS OF RESIDUAL STRESSES DURING COLD WORKING

[1]Prithvi Raj Arora
[1]Jeffrey Tan Meng Lee
[1]Christian Barnard
[2]Waqar Asrar

[1]Division of Aerospace Materials & Structures,
[2]Division of Fluid Mechanics & Aerodynamic,
Department of Aerospace Engineering,
Faculty of Engineering,
Universiti Putra Malaysia,
43400 UPM, Serdang,
Selangor Darul Ehsan, Malaysia.

ABSTRACT

A two-dimensional finite element (FE) analysis, under plane stress condition has been carried out using 2024-T351 aluminium alloy plate 6.35 mm thick with 6 mm diameter hole subjected to internal pressure. The material for the analysis is assumed to be isotropic, and a von Mises failure criterion along with linear isotropic hardening is used. The residual stress distribution has been obtained with pressure loading. The results indicate that large compressive tangential residual stresses were induced at the hole edge. Reverse yielding was observed for the pressure loading $P/\sigma_y > 1.2$. A linear relationship has been observed between the applied ND-pressure and the anticipated equivalent cold work till a ND-pressure of 1.2. A polynomial relationship is obtained giving the estimate of elastic-plastic boundary for a specified value of ND-pressure at the hole periphery.

Keywords: *Cold work, residual stress, elastic-plastic boundary, reverse yielding, finite element analysis, aluminium alloy.*

1.0 INTRODUCTION

Cracks emanating from fastener holes are a major cause of fatigue failure of aircraft components/structures. As a result, special manufacturing processes and mechanical treatments have been devised to alleviate the problem. One of these, cold working, is now commonly used in the aircraft industry. The cold working induces compressive residual stress around the hole region by inserting an oversized mandrel through the hole. The compressive residual stress field around the rim of the hole is responsible for delaying crack initiation and subsequently reduces crack growth rate to enhance the fatigue life of components [1, 2]. Since cold working has assumed a major importance for implementing fracture control plans in aerospace industry, both analytical and experimental assessment of the cold working technique are required.

Many theoretical analyses have been carried out for the solution of a hole in a finite width specimen loaded by radial pressure or enlargement, but only few solutions exist for materials considering strain-hardening property. Thus numerical methods and experimental technique have to be used to obtain the stress field in a number of practical components with finite size e.g. lugs. Hsu and Forman [3] studied the applicability of J_2 deformation theory for a pressurized hole in an infinitely large specimen using Budiansky's criterion [4]. Before this Mangasarian had carried out numerical analyses on the basis of J_2 deformation and incremental theories [5]. He found that the J_2 deformation theory is completely satisfied in the case of normally loaded circular holes. Moreover, the numerical solutions of the two theories do not differ greatly even when the stress paths are far from being radial. Recently Guo Wanlin [6] has developed an exact solution, using Budiansky's theory [7] for a finite circular sheet having a hole subjected to internal pressure, interference fit load as well as cold-worked stresses with the strain hardening behaviour and Bauschinger's effect. Subsequently Arora and Simha [8] have developed a closed form solution to evaluate the extent and movement of elastic-plastic front, considering both elastic strain and strain hardening effects. The elasto-plastic solution for a plate specimen with a hole subjected to internal pressure is developed using the modified Nadai's auxiliary variable and von Mises yield criterion. It is observed that for a specified elasto-plastic boundary the displacement at the edge of the hole varies linearly with pressure. It is also observed that with increase in strain hardening, the pressure required is higher and the corresponding displacement at the edge of the hole is smaller in magnitude. Normally the cold working in the rivet holes is understood by radial expansion of the holes when the process is carried out experimentally. In this investigation the cold working is done indirectly by the application of pressure at the hole periphery. Hence it is felt that an analysis is required relating the pressure loading with the anticipated cold work.

It is proposed to carry out an elastic-plastic finite element analysis in plane stress for an infinitely large plate with a hole subjected to internal pressure. Also it is required to develop a model to assess the extent of cold work using the results of this investigation.

2.0 MATERIAL PROPERTIES AND METHODS

A two-dimensional non-linear finite element analysis is carried out by using a general finite element code LUSAS-ANALYSTS to study the effect of pressure loading on the hole periphery of 2024-T351 aluminium alloy plate [9]. The plate specimen is of 6.35 mm thickness with a 6mm-diameter hole and is subjected to various levels of cold work through the application of internal pressure P on the surface of the hole.

The following power law relationship is used to define the material behaviour.

$$\varepsilon = \frac{\sigma}{E} \qquad for \qquad \sigma \le \sigma_y \tag{1}$$

and

$$\varepsilon = \frac{1}{E}\left(\frac{\sigma^{n+1}}{\sigma_y^n}\right) \qquad for \qquad \sigma \ge \sigma_y$$

The strength properties of 2024-T351 aluminium alloys have been taken from a handbook [10] and are given as follows:

Young's Modulus, E = 71.6 GPa
Uniaxial tensile yield strength, σ_y = 365 MPa
(0.1% proof stress in rolling direction)
Ultimate tensile strength, σ_{ut} = 510 MPa
Poisson's ratio, ν = 0.28
Mass density, $\rho = 2.78 \times 10^{-6}$ kg/mm^3
Strain hardening exponent, n = 9.1

Using above properties and the power law relationship equation (1), the discrete material data points were calculated to represent the non-linear true stress-strain behaviour (Figure 1). These data points are utilised in the FEM code to characterise the material behaviour. Stress Potential (Von Mises) material model is used for the present elastic-plastic finite element analysis [9].

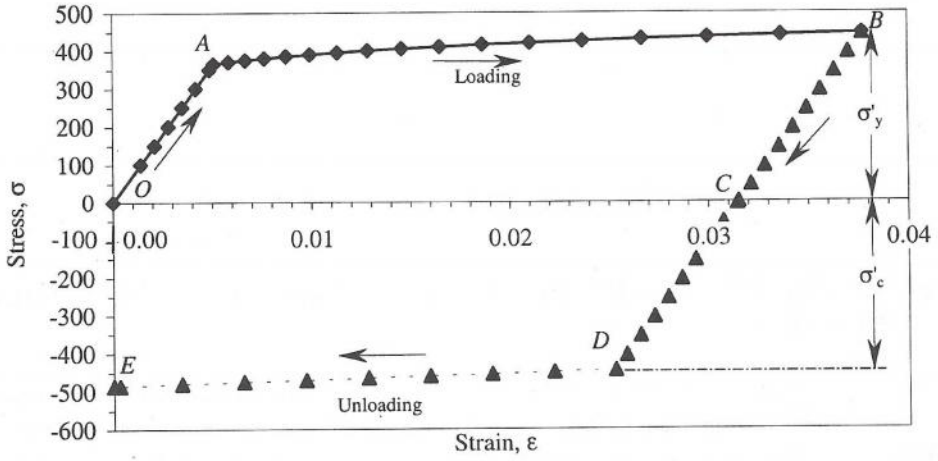

Figure 1 Stress-strain behaviour of 2024-T351 aluminium alloy representing isotropic hardening model used in finite element analysis

For the present analysis isotropic behaviour of the material is assumed. For the unloading case a negative pressure has been applied or in other words the maximum pressure at the hole edge has been slowly reduced from its maximum pressure value to zero pressure value. For carrying out the elastic-plastic analysis

as a whole the LUSAS software assumes that the compressive stress σ'_c represented by the point D is equal to that of tensile stress, σ'_y represented by the point B for isotropic hardening model (Figure 1). Also the software assumes an approximate straight line, represented by DE in the compressive region, behaviour in the inelastic region with a slope equals to that of the approximate slope of the straight line AB in the tensile region. This slope happens to be equal to 1.6 GPa. We are aware that most of the aluminium alloys do have the Bauschinger's effect and it does affect the final outcome of the analysis but due to the limitations of the LUSAS finite element software used in the present analysis we could not incorporate this effect.

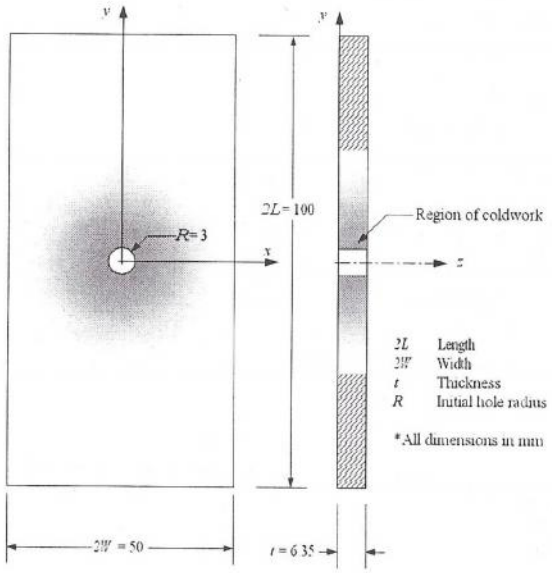

Figure 2 Model specimen details

3.0 MODEL GEOMETRY, BOUNDARY CONDITIONS AND LOADING DETAILS

The geometrical details of the 2024 T351 aluminium alloy plate specimen used to simulate cold-expansion of fastener hole are given in Figure 2. The symmetric nature of the model permits construction of a quarter model for the analysis (Figure 3). All the models are built using conventional 2D plane stress solid continuum element with enhanced strains (QPM4M), which is a rectangular element with 4-nodes from family of 2D isoparametric elements with fine integration scheme of 2×2 [9]. Under plane stress condition the stress behaviour around the hole is presumed to be independent of thickness z [11]. The mesh consists of 1725 QPM4M elements in the model (Figure 3). Around the hole region the mesh is refined to increase the density of the elements to reflect the

true nature of stress variations around the region for better results. The nodes along the y-axis and x-axis are restrained to move in the X and Y directions respectively.

The cold working simulation was carried out by incrementing the pressure value at the nodes in the radial direction to represent loading, and subsequently reverse the direction of pressure loading from its maximum value until the pressure loading becomes zero at the respective nodes to represent the complete unloading. Both automatic and manual loadings are utilised for the present analysis. Automatic loading is used for loading phase, whereas the manual loading is used for the unloading phase. The initial pressure corresponding to the yielding at the hole edge is obtained after a few trials in the elastic region of the loading and this pressure is termed as the incipient pressure. This incipient pressure happens to be approximately equal to 200 MPa. From this pressure onwards the analysis in the inelastic region is carried out. Hence uniform pressure load P was selected in the range from 200 MPa to 700 MPa. These load values were assigned to the hole perimeter to simulate various degrees of cold working.

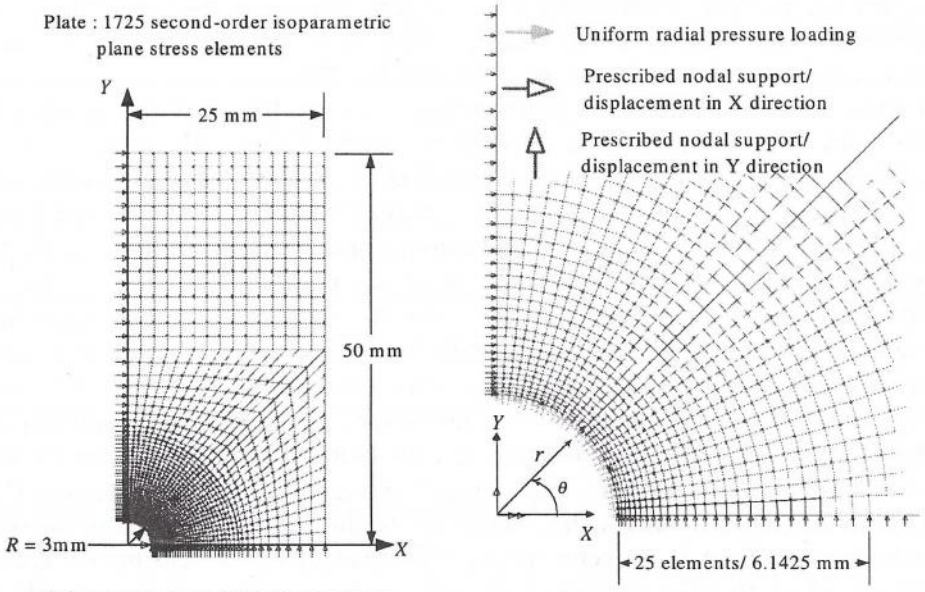

(a) Overall FE mesh of quarter specimen

(b) Detailed view of the mesh around the hole region

Figure 3 Two-dimensional FE model with uniform radial pressure loading along the hole perimeter

4.0 RESULTS AND DICUSSIONS

The non-dimensional (ND) tangential stress, $\sigma_{\theta\theta}/\sigma_y$ and ND-radial stress, σ_{rr}/σ_y distribution as a function of the ND-radial distance, r/R from the hole edge for loading and unloading cases for various ND-pressure, P/σ_y levels ranging from

0.6 to 1.9 is given in Figures 4 to 5. Several ND-pressure loads, $0.5 < P/\sigma_y < 0.6$, have been applied to check the incipient yielding at the hole edge and thereby to find out the corresponding pressure. It is observed that this value of P/σ_y is approximately 0.5778. For ND-pressure, $P/\sigma_y = 0.5778$ the ND-tangential stress, $\sigma_{\theta\theta}/\sigma_y$ decreases from the hole edge with radial distance (Figure 4a). The maximum value of ND tangential stress, $\sigma_{\theta\theta}/\sigma_y$ is 0.5865 at the hole edge for P/σ_y equals to 0.5778.

The maximum ND tensile tangential stress, for an individual curve, and the applied ND pressure at the hole periphery represents the elastic-plastic interface (Figure 4a). The maximum ND-tensile tangential stresses at the elastic plastic interface $r_{e\text{-}p}$ are about the same for all ND-pressure values (Figure 4a). The outward radial movement of elastic plastic interface $r_{e\text{-}p}$ as the pressure increases designates a progressive spreading of plastic zone in radial direction. Beyond the elastic plastic interface $r_{e\text{-}p}$ the ND-tangential stress gradually decreases for the loading case till the external boundary of the plate specimen is reached.

The ND-radial stress at the hole edge increases, in its absolute value, as the ND-pressure increases (Figure 4b). It has been observed that the non-dimensional radial stress distribution remains compressive in nature for the whole radial domain for the set of non-dimensional pressures studied.

Figure 5a shows the ND-tangential residual stresses for an unloading case for various pressures. An immediate effect of unloading, for the cold worked hole, is the redistribution of ND-stresses. The ND-tangential residual stresses are compressive near the hole edge, and they gradually become tensile before elastic plastic interface $r_{e\text{-}p}$ is reached and remains completely tensile in nature till the external boundary of the specimen is reached (Figure 5a). The size of compressive stress region responsible for enhancing the life of a specimen/ component during service loading depends primarily on the amount of cold work subjected to the material. On the contrary to the almost constant peak ND-stresses observed at elastic plastic interface $r_{e\text{-}p}$ during loading phase, the amount of peak ND-stresses at elastic plastic interface $r_{e\text{-}p}$ for unloading phase tend to steadily rise (Figure 5a). The maximum peak stress is achieved for pressure loading $P/\sigma_y = 1.9$ in current analysis, which corresponds to the maximum applied pressure. The reverse yielding is reflected in the ND residual stress distribution curves upon unloading by a flat portion of the curve starting from the hole edge till the second elastic-plastic boundary in the radial direction (Figure 5a).

The ND-radial residual stresses are equal to zero at the hole edge and increase in a compressive manner to their maximum values at a certain distance from hole edge and then subsequently decrease with ND-radial distance (Figure 5b). Similar to ND-tangential residual stresses, the magnitude of radial residual stress depends on the level of cold expansion. For a ND-pressure loading $P/\sigma_y > 1.2$ the reverse yielding occurs. The occurrence of reversed yielding reduces the magnitude of compressive tangential stress at the hole edge.

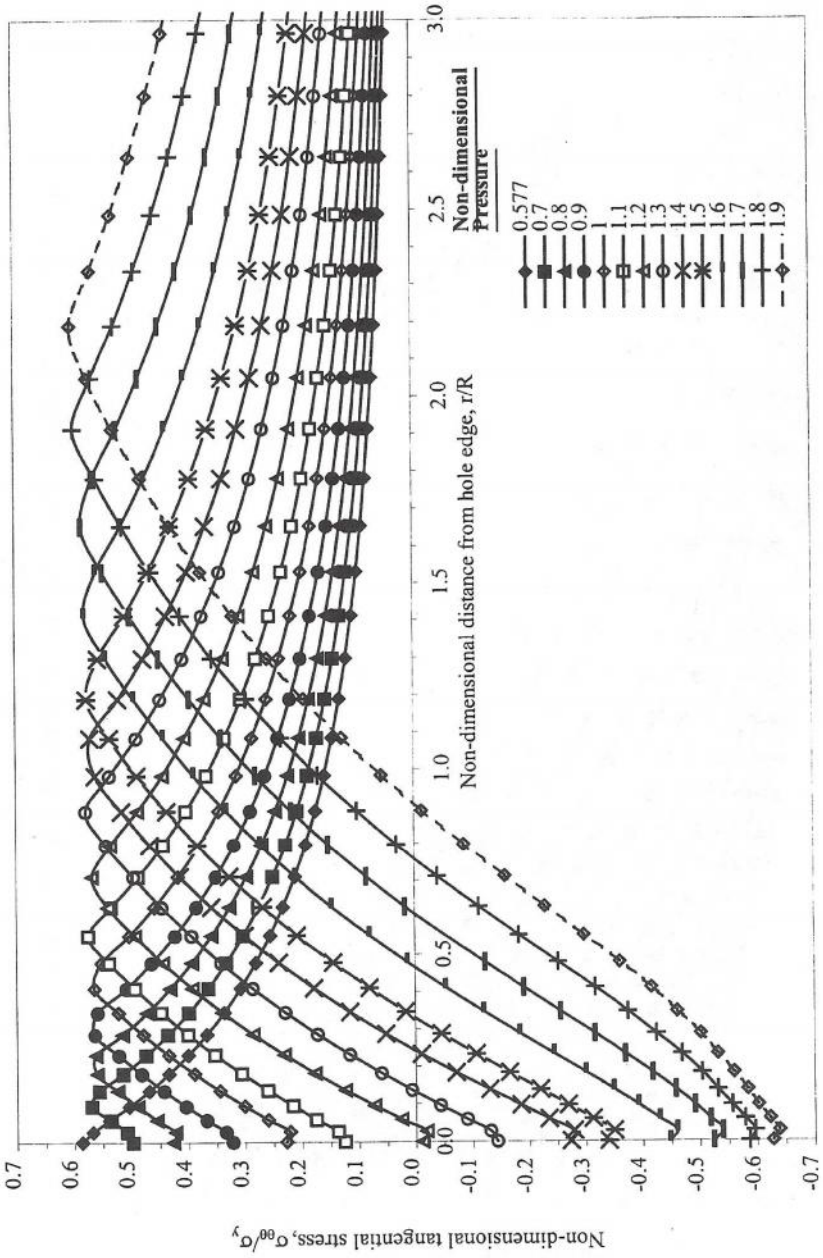

Figure 4a Non-dimensional tangential stress versus non-dimensional radial distance from the hole edge (loading case)

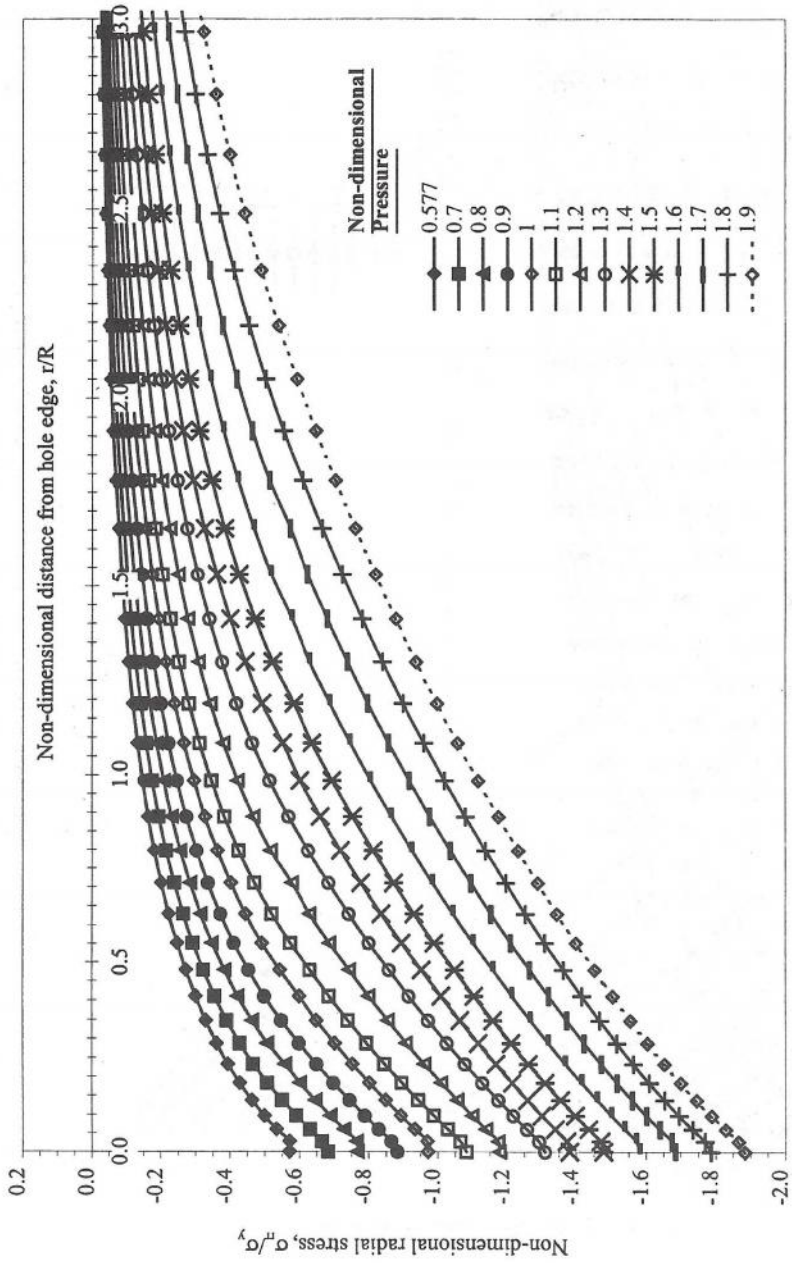

Figure 4b Non-dimensional radial stress versus non-dimensional radial distance from the hole edge (loading case)

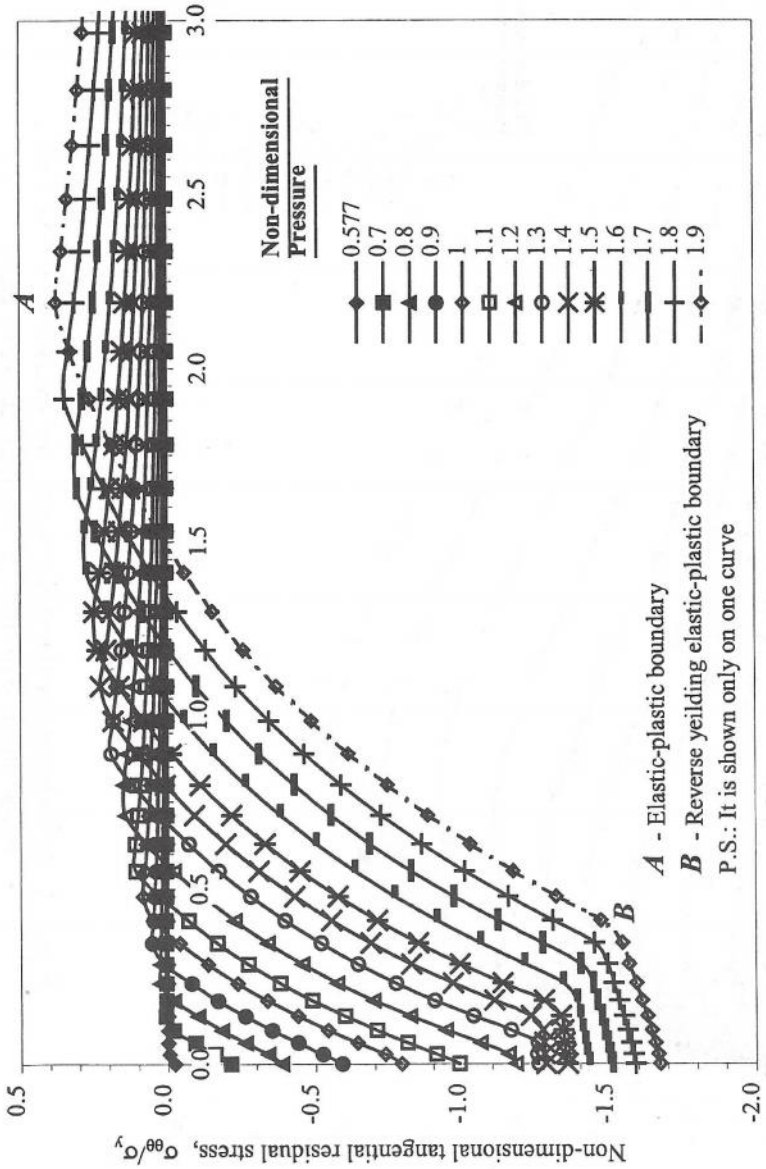

Figure 5a Non-dimensional tangential residual stress versus non-dimensional radial distance from the hole edge (unloading case)

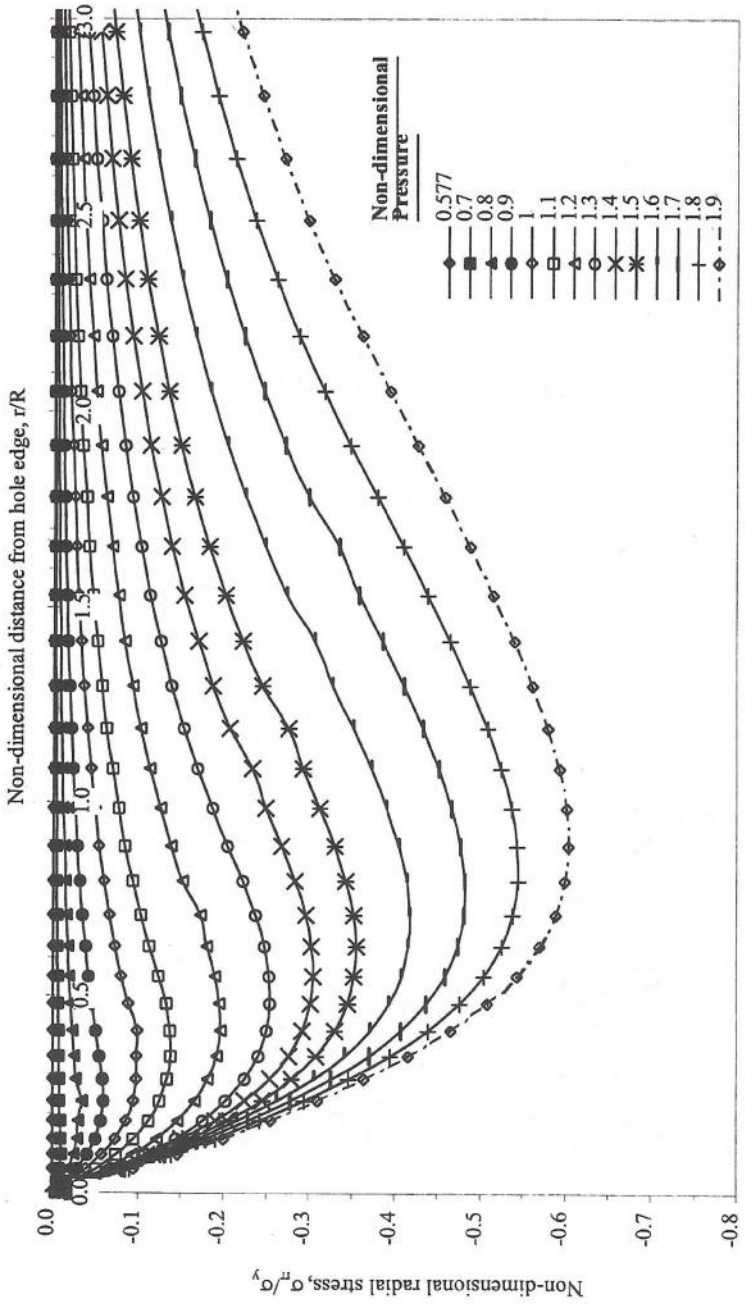

Figure 5b Non-dimensional radial residual stress versus non-dimensional radial distance from the hole edge (unloading case)

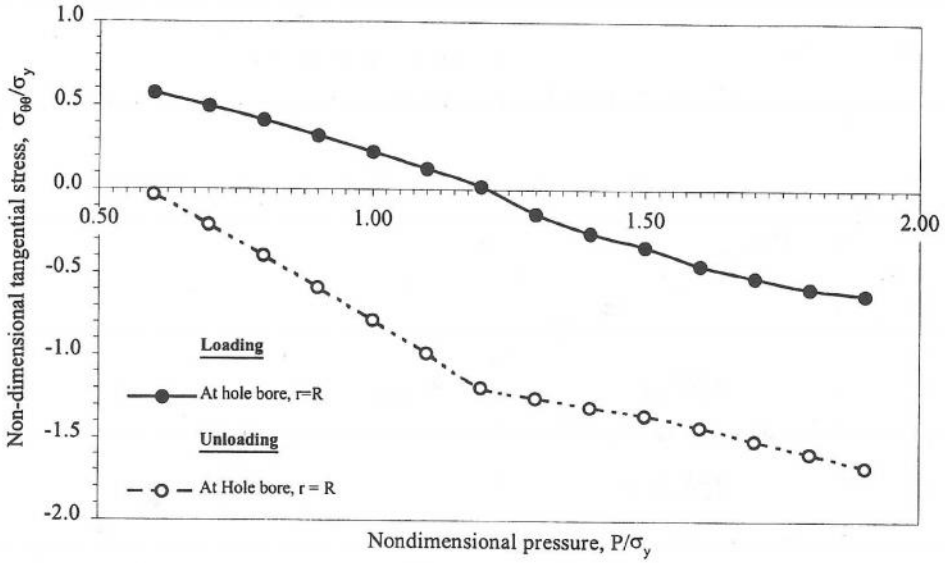

Figure 6a Non-dimensional tangential stress at hole edge versus non-dimensional pressure

From the data shown in Figure 4a the value of the ND tangential stress at the hole edge is obtained for the loading case and is drawn against the ND pressure loading (Figure 6a) as a solid line. In the same way from the data shown in Figure 5a, the value of residual ND tangential stress at the hole edge is obtained for the unloading case and is drawn against the ND pressure loading (Figure 6a) as a dotted line. As the applied pressure loading, P/σ_y increases; the corresponding non-dimensional tangential stress $\sigma_{\theta\theta}/\sigma_y$ at the hole edge decreases gradually from its tensile value of 0.5865 for P/σ_y equals to 0.5778 and goes to its maximum compressive value -0.6269 for P/σ_y equals to 1.9 (Figure 6a). This corresponds to the loading phase of the analysis. Each point on the solid line in Figure 6a represents a different set of analysis carried out for different ND pressure loadings (Figure 4). The first point on the solid line corresponds to the incipient yielding and upon unloading this gives zero residual stresses, which is shown on the abscissa of the curve as the starting point of the dotted line curve. The points on the dotted line in Figure 6a represents the data of residual ND tangential stresses at the hole edge after unloading corresponding to the points shown on the solid line given for the loading case.

The ND-radial stress, σ_{rr}/σ_y data for the loading and the unloading cases for the different ND pressure, P/σ_y are obtained from Figures 4b and 5b, and are drawn as a solid line and a dotted line respectively in Figure 6b. The ND-radial stress, σ_{rr}/σ_y at the hole edge for the loading case increases in its absolute value with ND-pressure loading. The residual ND radial stress decreases to its zero stress value upon unloading. The radial stress in a way is equal to the applied pressure, so as the pressure is removed from the hole edge the radial stress is also removed and hence its value becomes zero.

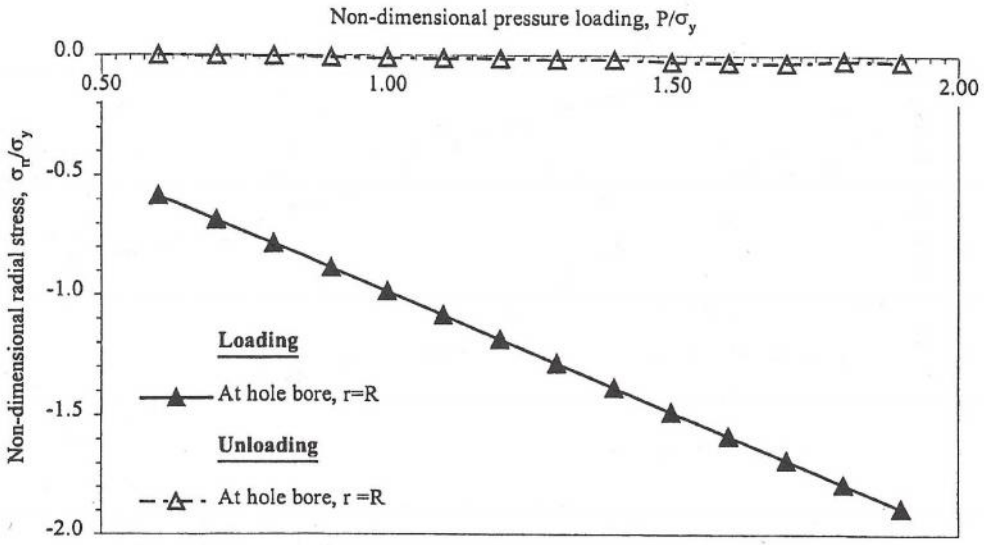

Figure 6b Non-dimensional radial stress at the hole edge versus non-dimensional pressure

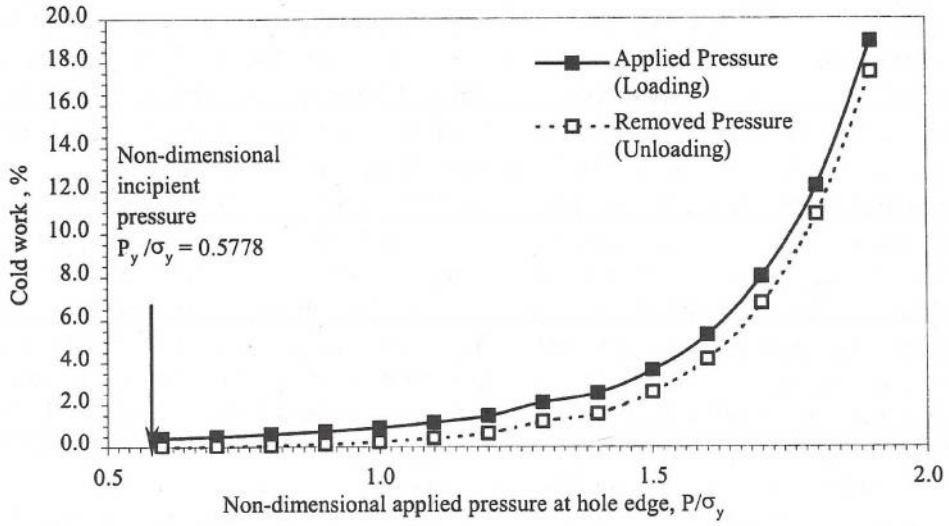

Figure 7 Non-dimensional pressure versus cold work

Each set of data points in Figure 7 corresponds to a separate analysis. The solid point on the solid line represents the equivalent cold work experienced at the hole edge, while a hollow point on another dotted line represents the residual equivalent cold work experienced at the hole edge. Figure 7 gives the functional

relation between the applied pressure and the corresponding equivalent amount of cold work during the loading phase and the unloading phase. The cold work is applied to the specimen through the pressure loading in this analysis and the implied equivalent cold work on the hole expansion basis is defined and calculated by the following relation:

$$\text{Percent cold work} = \frac{D_f - D_i}{D_i} \times 100 \tag{2}$$

A linear relationship between the applied pressure and the anticipated equivalent cold work is observed till a pressure loading of 1.2. Further the anticipated equivalent cold work increases nonlinearly for the subsequent increase in pressure.

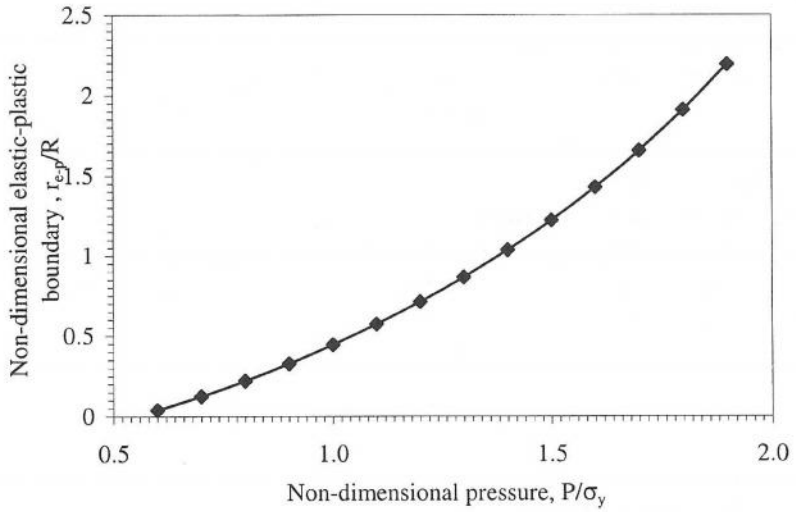

Figure 8 Non-dimensional pressure versus non-dimensional elastic-plastic boundry

Figure 8 gives an estimate of the elastic-plastic boundary from the hole edge for the given applied pressure and is approximated by the following polynomial relation using least squares fit method,

$$\left(\frac{r_{e-p}}{R}\right) = 0.4643 \cdot \left(\frac{P}{\sigma_y}\right)^4 - 1.4619 \cdot \left(\frac{P}{\sigma_y}\right)^3 + 3.2479 \cdot \left(\frac{P}{\sigma_y}\right)^2$$

$$- 0.2925 \cdot \left(\frac{P}{\sigma_y}\right) - 0.6229 \tag{3}$$

where,

P is the pressure applied at the hole edge
σ_y is the yield strength of the material
$r_{e\text{-}p}$ is the elastic-plastic boundary measured from the hole edge, and
R is the radius of the hole.

The polynomial equation (3) is to be used for developing fatigue life prediction models for aerospace applications.

5.0 CONCLUSIONS

The following conclusions are deduced from the finite element analysis carried out for cold working process for 2024-T351-aluminium alloy using finite element software LUSAS-ANALYST.

1. The simulation results indicate that large compressive tangential residual stresses are induced at the hole edge upon unloading.
2. Reverse yielding is observed if the pressure loading, P/σ_y is greater than 1.2 and it is reflected in the stress distribution after unloading giving second elastic-plastic boundary.
3. A linear relationship is observed for the applied ND pressure, P/σ_y and the anticipated equivalent cold work for a ND pressure loading of 1.2.
4. A polynomial relationship is developed giving the estimate of elastic-plastic boundary for an applied ND- pressure.

NOMENCLATURE

D_f	Hole diameter after cold working
D_i	Initial hole diameter
E	Modulus of elasticity
n	Strain hardening exponent
P	Applied pressure at the hole periphery
P_y	Pressure that causes yielding at the hole periphery
R	Hole radius
r	Instantaneous radius
$r_{e\text{-}p}$	Elastic-plastic boundary in radial direction from the hole edge
ε	Strain
σ	Stress

Subscripts

θ	Tangential direction
r	Radial direction
y	Yield
c	Compressive

ACKNOWLEDGEMENT

The authors gratefully acknowledge the financial support of Ministry of Science, Technology & Environment, Malaysia (IRPA Project No. 03-02-04-0089), for the provision of a research grant for this work.

REFERENCES

1. Fatigue Technology Inc., 1991, "*Extending the Fatigue of Metal Structures*, Materials Testing, FATIGUE TECHNOLOGY INC., 150 Andover Park West, Seattle, Washington, USA.
2. Fatigue Technology Inc., FTI PROCESS SPECIFICATION 8101C – July 28, 1994, *Cold Expansion of Holes Using the Standard Split Sleeve System and Countersink Cold Expansion* $_{TM}$ *(Cs Cx* $_{TM}$*)*.
3. Hsu, Y. C. and Forman, R. G., June 1975, "Elastic-plastic analysis of an infinite sheet having a circular hole under pressure", *ASME Journal of Applied Mechanics*, pp.347-352.
4. Budiansky, B., June 1959, "A reassessment of deformation theories of plasticity", *ASME Journal of Applied Mechanics*, pp.259-264.
5. Mangasarian, O. L., March 1960, "Stresses in the plastic range around a normally loaded circular hole in an infinite sheet", *ASME Journal of Applied Mechanics,* pp.65-73.
6. Guo Wanlin, 1993, "Elastic-Plastic Analysis of a Finite Sheet with a Cold-Worked Hole", *Engineering Fracture Mechanics*, Vol.45, No.6, pp.851-864.
7. Budiansky, B., 1971, "An exact solution to an elastic-plastic stress concentration problem", *Prikl. Mat. Physics*, Vol. 35, pp.40-48.
8. Arora, P. R. and Simha, K. R. Y., 1996, "Analytical and experimental evaluation of coldworking process for strain hardening materials", *Engineering Fracture Mechanics*, Vol. 53, No.3, pp.371-385.
9. LUSAS (London University Stress Analysis System), 2001, FEA Ltd Forge House, 66 High Street, Kingston upon Thames, Surrey, KT1 1HN, United Kingdom.
10. MIL-HDBK-5D (McDonnell Douglas Corporation): *Military Standardisation Handbook, Metallic Elements for Aerospace Vehicle Structures*, 1985, Vols. 1 & 2, 3.91
11. Timoshenko, S. P and Goodier, J. N., 1982. *Theory of Elasticity*, McGraw-Hill International, 15-16.